The critical stress criterion for gaseous hydrogen embrittlement

P. DOIG, G. T. JONES
Central Electricity Generating Board, South Eastern Region, Scientific Services Department, Gravesend, Kent, UK

A criterion for susceptibility to hydrogen embrittlement based on the development of a critical hydrostatic stress has been proposed. The hydrostatic stress distribution ahead of plastically strained notches has been described analytically and correlated with measured susceptibility to hydrogen embrittlement. The predictions of the analysis are in good agreement with available experimental data and support the critical stress criterion for hydrogen embrittlement.

1. Introduction

The embrittlement of high strength steels by gaseous hydrogen or hydrogen-containing atmospheres is a well established phenomenon which has led to a number of engineering failures [1–6]. These have generally been associated with operation in high-pressure hydrogen environments but more recently, failures have occurred in low-pressure environments, < 1 MPa [1], and laboratory specimens have failed by such embrittlement at pressures down to $\simeq 1$ Pa [7–11].

There have been a number of theories proposed to explain the observed embrittling effect of hydrogen, most of which, however, are based on the original proposals of Troiano and co-workers [11, 12]. These investigators put forward the concept of a long-range diffusion of hydrogen to the triaxial stress-field developed ahead of a stressed notch or crack. Since then, this concept has been extended to include failure mechanisms based on void information [13] by hydrogen precipitation, reduction of the cohesive strength of the metal–metal bond [13, 14] and surface energy considerations involving a lowering of the Griffiths fracture energy [15, 16] by adsorption of hydrogen. Whatever the detail of these various models, they all require the development of a critical concentration of hydrogen and, according to Troiano [12], this concentration is developed by the stress-induced segregation of hydrogen to the regions of high triaxial stress. Such theories, therefore, all suggest that susceptibility to hydrogen embrittlement in a given environment is associated with the development of a critical hydrostatic stress. Indeed, a recent analysis [10] based on such a concept has successfully predicted the kinetics of embrittlement of notched steel specimens in hydrogen gas environments. Such a criterion is difficult to establish when applied to crack geometries for two reasons. Firstly, at present the precise form and magnitude of the stress distribution ahead of a plastically strained crack are not available. Secondly, it is generally accepted in notch fracture studies that in order to initiate cracking it is not only necessary to achieve a critical stress or strain but that it must also be developed over a microstructural distance which is appropriate to the failure mechanism involved [17–23]. For cracks, the stress gradients are contained within only a few micrometres such that in many materials they are confined to within one grain and the peak stresses to within only fractions of a grain. Consequently, for failure processes which require a critical stress over microstructural dimensions which are significant with respect to the extent of the stress field, the applied loads for continued cracking will vary with the relative position and orientation of the crack and the local crack tip microstructure. For blunt notches, however, where the notch root radius is large relative to microstructural dimensions, stress gradients are shallow and the peak stresses occur over distances which are large such that local fine-scale microstructural influences will not predominate. Thus, for blunt notches, the concept of a critical hydrostatic stress for failure which is characteristic of the general microstructure will be applicable.

The purpose of the present work is to derive an analytical description of the hydrostatic stress field ahead of plastically strained notches and compare this with their measured hydrogen embrittlement behaviour in a gaseous hydrogen-containing environment and thus establish the validity of a critical stress criterion.

2. Hydrostatic stress criterion for hydrogen embrittlement

The interaction, U, controlling solute segregation in a stress field is given by [24]:

$$U = p\Delta V \tag{1}$$

where p is the pressure tensor of the stress field and ΔV is the change in atomic volume due to the insertion of a solute atom. This increases the equilibrium solute concentration, C_x, at any point, x, within the stress field given by [25]:

$$C_x = C_0 \exp\left[\frac{p\Delta V}{kT}\right], \tag{2}$$

where C_0 is the equilibrium concentration in the absence of stress, k is Boltzmann's constant and T is the absolute temperature. This may be given as [26]:

$$C_x = C_0 \exp\left[\frac{\sigma_i V_H}{3RT}\right] \tag{3}$$

where V_H is the partial molar volume of hydrogen, R is the gas constant, ($= kN$ where N is the Avogadro number), σ_i is the summation of the principal stresses such that $\sigma_i/3$ is the hydrostatic component of the applied stresses. Consequently, the attainment of a critical hydrogen concentration is associated with the development of a critical hydrostatic stress.

The hydrostatic stress distribution ahead of a notch in plane strain is shown schematically in Fig. 1. For plane strain and assuming a perfectly elastic–plastic solid with no work-hardening, we may use Hill's [27] slip-line field equation for the hydrostatic stress in the "plastic zone" immediately ahead of a notch of radius r given by [28]:

$$\sigma_i/3\ (\text{plastic}) = \sigma_y\ \{\ln(1 + x/r) + \tfrac{1}{2}\} \tag{4}$$

where σ_y is the material's yield stress and x is the

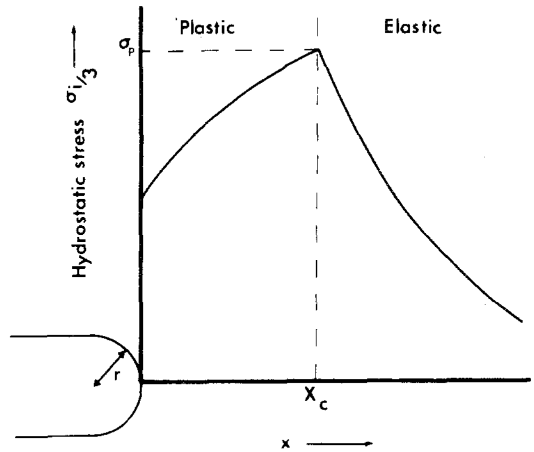

Figure 1 Schematic diagram showing the distribution of hydrostatic stress ahead of a plastically deformed notch.

distance ahead of the notch. When the plastic zone size is small the distribution of hydrostatic stress in the "elastic" regime may be assumed, for simplicity, to be unaltered by the plastic yielding at the root of the notch. For blunt notches where $r \simeq a$ (the notch depth) the distribution of elastic hydrostatic stress ahead of a stressed notch may be approximated to [29]:

$$\sigma_i/3\ (\text{elastic}) = \sigma_{\text{nom}}\{(1+\nu)/3\} \times \{1 + (K_t - 1)/(1 + x/r)^3\} \tag{5}$$

where σ_{nom} is the nominal applied stress, ν is Poisson's ratio and K_t is the elastic stress intensification factor for the particular notch geometry. The position x_p, and value of the maximum hydrostatic stress, σ_p, in Fig. 1 may be obtained by combining Equations 4 and 5 to give a peak hydrostatic stress, σ_p, of:

$$\sigma_p = \sigma_{\text{nom}}\ \{(1+\nu)/3\} \times \{1 + (K_t - 1)/[\exp(\sigma_p/\sigma_y - \tfrac{1}{2})]^3\}. \tag{6}$$

In reality, stress redistribution and work-hardening will affect these stress profiles. Comparison with available finite element analyses for sharp notches, however, indicates that these equations give good approximations to the real profiles.

Associated with the hydrostatic stress profile ahead of a plastically strained notch is an equilibrium hydrogen concentration which is given by combining Equations 3, 4 and 5. The time-dependence for hydrogen segregation to produce this profile is reflected in the initiation time for cracking [10, 12, 22, 26, 30, 31].

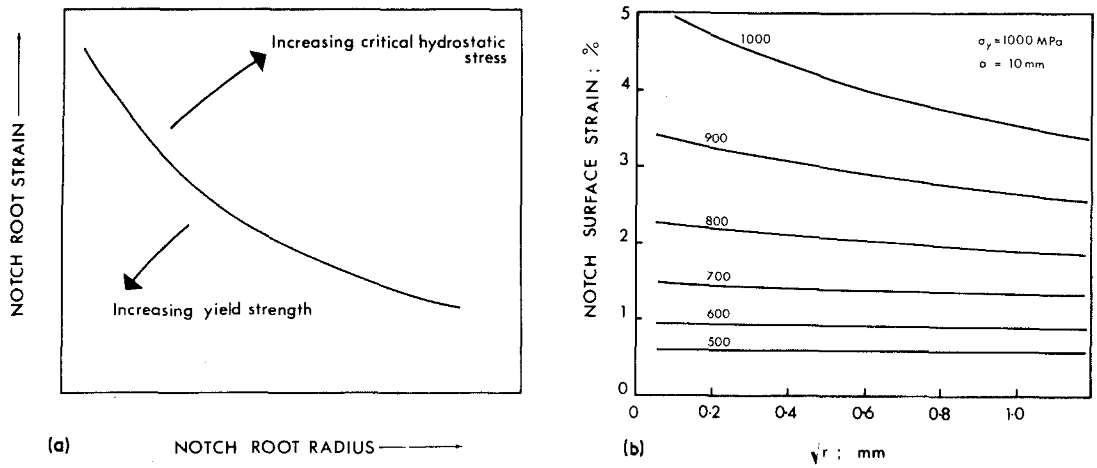

Figure 2 Plots of notch surface strain (elastically calculated) as a function of notch root radius for: (a) general case – schematic, (b) a high-strength alternator end-ring steel with a range of peak hydrostatic stresses and $\sigma_y = 1200\,\mathrm{MN\,m^{-2}}$.

The elastically calculated notch surface strain, ϵ, at the root of a loaded notch is given by:

$$\epsilon = (K_t \sigma_{nom}/E) \tag{7}$$

where E is Young's modulus. Thus for any given peak hydrostatic stress, σ_p, we obtain a relationship between the surface strain, ϵ, and the notch geometry by combining Equations 6 and 7 to give:

$$\epsilon = (K_t \sigma_p/E)\,[\{(1+\nu)/3\} \times \{1 + (K_t - 1)/[\exp(\sigma_p/\sigma_y - \tfrac{1}{2})]^3\}]^{-1}, \tag{8}$$

where K_t is a function of the notch geometry. For the case of a single notch in an infinite sheet the elastic stress intensification factor is given by [32]:

$$K_t = 1 + 2\sqrt{(a/r)} \tag{9}$$

where a is the notch depth. Consequently, from Equations 8 and 9 we obtain an analytical relationship between the notch geometry notch surface strain, peak hydrostatic stress and material yield strength. The general characteristics of this relationship are shown schematically in Fig. 2a together with a specific plot for a high strength end-ring steel in Fig. 2b. For any fixed value of $\sigma_p > \sigma_y/2$ (i.e. some plasticity), the elastically calculated notch surface strain, ϵ, is not independent of the notch geometry but increases with decreasing notch root radius and increasing notch depth, i.e. increases with increasing value of K_t (Equations 8 and 9).

3. Experimental test of critical hydrostatic stress criterion

The results of the analysis described in Section 2 clearly show that a critical hydrostatic stress criterion for gaseous hydrogen embrittlement of notched geometries predicts a change in the elastically calculated surface strain at failure for different notch geometries. The notch geometry may be characterized by the elastic stress intensification factor, K_t, which is a function of the notch depth and root radius.

Most of the available data relating to the failure of notched samples by gaseous hydrogen embrittlement have been obtained on laboratory specimens loaded in such a way as to introduce a significant degree of mode 1 bending stress. These include variously notched Charpy specimens loaded in three or four-point bending where loading is pure bend, and notched CK type specimens where loading is a mixture of tension and bending. Any bending contribution in the loading effectively introduces a non-uniform distribution of nominal stress, σ_{nom}, ahead of the notch. This is illustrated schematically in Fig. 3a and b. The distribution of nominal stress ahead of the notch may be given as:

$$\sigma_{nom} = \sigma_{nom\,(x=0)}\{1 - \alpha x\,(w-a)\} \tag{10}$$

where $(w - a)$ is the net section of the notched specimen and α is the numerical factor which defines the relative contributions of bending and tensile loading on the specimen. For pure bending $\alpha = 2$, whereas for pure tension, $\alpha = 0$. As a result of this distribution of nominal stress ahead of the

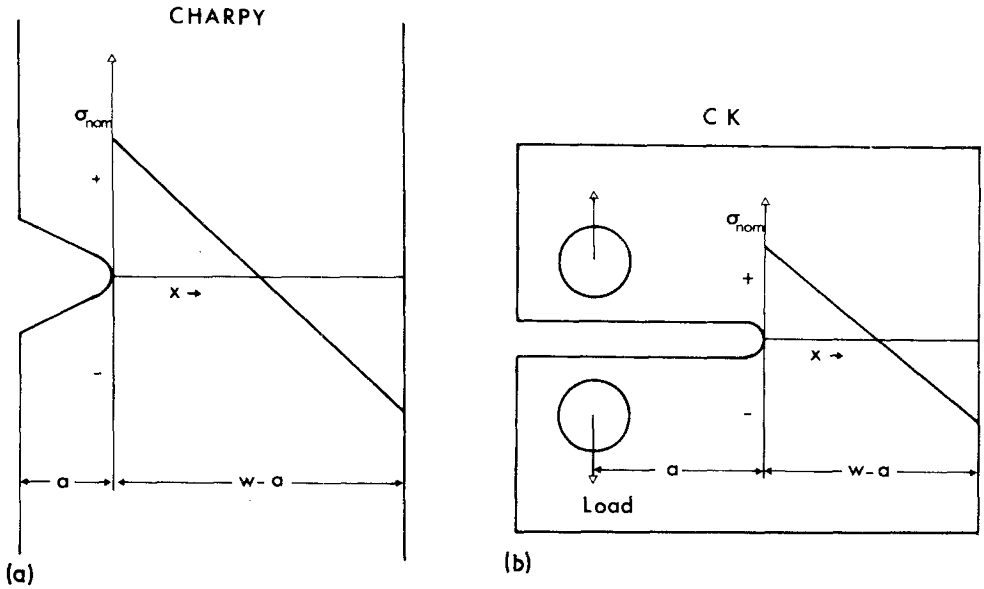

Figure 3 Schematic diagram showing the distribution of nominal stress ahead of the notch in: (a) a Charpy bend specimen and, (b) a CK specimen.

notch, the development of a critical elastic hydrostatic stress ahead of the notch requires an increase in the elastically calculated stress at the notch root. Thus the term σ_{nom} in Equation 7 must be replaced by $\sigma_{nom\,(x=0)}$ in Equation 10. Substituting for x_p from Equation 4 gives:

$$\epsilon = (K_t\sigma_p/E)\left[\{(1+\nu)/3\}* \{1+(K_t-1)/[\exp(\sigma_p/\sigma_y-\tfrac{1}{2})]^3\} \times\left(1-\{\alpha r[\exp(\sigma_p/\sigma_y-\tfrac{1}{2})-1]/(w-a)\right)\right]^{-1}. \quad (11)$$

The effect of the bending is to increase the elastically calculated surface strain required to develop a critical hydrostatic stress, σ_p, at the elastic–plastic interface, x_p. This increase becomes greater as K_t decreases, i.e. as the notch root radius increases. The value of K_t for notched Charpy and CK type test specimens is given by [33]:

$$K_t = 2K/\{\sigma_{nom}(\pi r)^{1/2}\}, \quad (12)$$

where K is the stress intensity factor for the given geometry. This expression may be evaluated to give:

$$\text{CK specimen } (a/w = 0.5) \rightarrow K_t = 3.83/\sqrt{r}$$

and

$$\text{Charpy bend } (a/w = 0.2) \rightarrow K_t = 1.776/\sqrt{r}, \quad (13)$$

for r measured in mm. For Charpy bend specimens the value of α in Equation 2 is $\simeq 2$. Similarly, the bend component of loading in the CK specimen is predominant and, consequently, α may be approximated to 2 in this case also.

The value of critical surface strain, ϵ, has been evaluated as a function of notch root radius for both Charpy and CK specimens of a high strength ferritic steel using Equations 11 and 12. Calculated plots for a ferritic steel with $E = 2.1 \times 10^5$ MN m^{-2} and $\sigma_y = 1200$ MN m^{-2} are shown in Fig. 4a and b for notched Charpy ($a/w = 0.2$) and CK ($a/w = 0.5$) specimens. Superimposed on these plots are experimental values obtained from a number of tests in dry hydrogen sulphide gas at different pressures [34]. In addition, Table I shows experimental data obtained at Westinghouse laboratories [35] on two 4340 ferritic steels with different values of yield strength together with calculated surface strains assuming a constant value of σ_p for each.

In general, the experimental values are in good agreement with the predictions of the present analysis in that the elastically calculated notch root strain increases as the notch root radius decreases (Fig. 4a and b). In addition, the results indicate a critical hydrostatic stress which increases with decreasing external pressure of the test environment (Fig. 3b), and increasing material yield stress (Table I).

TABLE I: (a) Experimental values for notch surface strains to initiate hydrogen embrittlement in notched CK specimens of 4340 high strength steels [35]

Steel	K_t	Notch root radius r (mm)	Notch depth a (mm)	Specimen width w (mm)	Notch strain (%) Measured	Notch strain (%) Calculated	Hydrostatic stress σ_p ($MN \cdot m^{-2}$)
A	23.1	0.08	19.5	64.77	3.58	3.52	
A	11.4	0.25	25.4	64.77	3.30	3.24	1100
A	3.33	1.27	38.1	64.77	2.26	2.43	
B	11.4	0.25	25.4	64.77	1.45	1.52	950
B	3.33	1.27	38.1	64.77	1.50	1.47	

(b) Specification of 4340 steels

	Yield strength σ_y ($MN\,m^{-2}$)	Composition (wt %) C	Mn	Ni	Cr	Mo	V
A	1241	0.36	0.63	2.54	0.86	0.39	0.09
B	1482	0.41	0.81	1.88	0.91	0.37	–

4. Discussion

This analysis presents a criterion for the development of susceptibility to gaseous hydrogen embrittlement based on the development of a critical hydrostatic stress. This stress reduces the local activity of dissolved hydrogen atoms resulting in the segregation of additional hydrogen to these regions. The increased local hydrogen concentration lowers the resistance to cracking such that in conjunction with the applied stress, a hydrogen embrittlement crack will initiate.

This model has been developed for cracking from a blunt notch where the plastic zone size and extent of the peak hydrostatic stresses are large compared with the scale of the microstructure. Consequently, the critical hydrostatic stress will represent a mean value which is characteristic of the material. Where the range of the peak hydro-

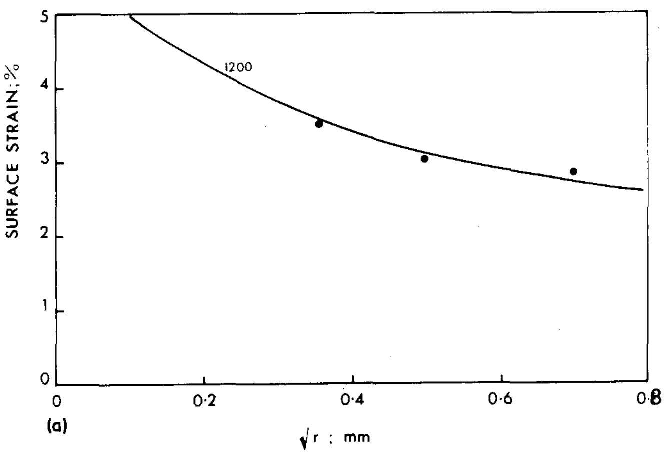

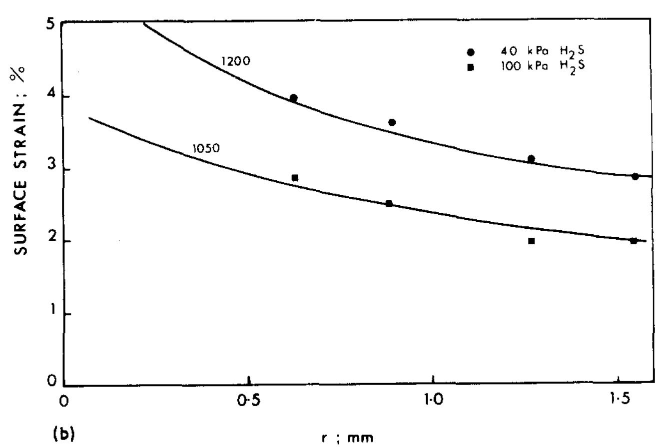

Figure 4 Calculated and experimental values of elastically calculated notch root strain for hydrogen embrittlement susceptibility in: (a) Charpy notch bend, $a/w = 0.2$, (b) CK notch tensile, $a/w = 0.5$, ferritic steel specimens with $\sigma_y = 1200\,MN\,m^{-2}$. Calculated values are for $\sigma_p = 1050$ and $1200\,MN\,m^{-2}$.

static stress is small relative to the scale of the microstructural feature which is associated with crack initiation, i.e. for small notch root radii, the analysis must be modified. In general, this will become important when the plastic zone size is of the same order as the microstructural feature associated with the crack initiation process. For ferritic steels this is generally very small $< 10\,\mu m$; but for typical austenitic steels, where the grain size is much larger ~ 1 mm, the effect may be significant, even for quite blunt notches. In general, however, the good agreement obtained between the predictions of this analysis and the available experimental data, supports the concept of a critical hydrostatic stress for initiation of hydrogen embrittlement cracking ahead of blunt notches. This analysis is necessary to evaluate the susceptibility of blunt notch geometries occurring in large engineering components where direct measurement is not possible using conventional laboratory-sized specimens.

The stress analysis adopted in this work is clearly an oversimplification of the true stress state since it takes no account of work-hardening or elastic stress redistribution as a result of plastic yielding at the notch tip. A complete analysis requires the use of iterative computer techniques. However, the general trends of this analytical approach are correct and enable us to examine the overall influence of each of the relevant variables.

5. Conclusions

(1) The gaseous hydrogen embrittlement susceptibility of high-strength steels may be interpreted in terms of the development of a critical hydrostatic stress.

(2) An analysis on the concept of a critical hydrostatic stress ahead of a stressed notch predicts an elastically calculated notch root strain for embrittlement which is a function of K_t.

(3) The notch root strain for embrittlement increases with increasing value of K_t, decreasing notch root radius, increasing critical hydrostatic stress and decreasing material yield strength.

Acknowledgement

This paper is published by permission of the Director General, Central Electricity Generating Board, South Eastern Region.

References

1. C. B. JOLLY, M. C. MURPHY, A. N. PATERSON and D. J. PETTY, Presented to CEA Thermal and Nuclear Power Section, Halifax, Nova Scotia (1975).
2. A. E. SCHEUTZ and W. D. ROBERTSON, *Corrosion* **13** (1957) 537.
3. L. W. VOLLMER *ibid* 8 (1952) 236.
4. R. S. TRESEDER, International Conference on Stress Corrosion Cracking and Hydrogen Embrittlement of Iron-Based Alloys, Unieux-Firminy, France (1973).
5. R. J. WALTER and W. T. CHANDLER, Western Metal and Tool Conference and Exposition (1969).
6. W. B. McPHERSON and C. E. CATALDO, Materials Engineering Exposition and Congress, Detroit (1962).
7. M. R. LOUTHAN, "Hydrogen in Metals", edited by I. M. Bernstein and A. W. Thomson (ASM, Metals Park, Ohio, 1974).
8. R. A. ORIANI and P. H. JOSEPHIC, *Acta Met.* **22** (1974) 1065.
9. G. G. HANCOCK and H. H. JOHNSON, *Trans. Met. Soc. AIME* **236** (1966) 513.
10. P. DOIG and G. T. JONES, *Met. Trans.* 8 (1977) 1933.
11. E. A. STEIGERWALD, E. W. SCHALLER and A. R. TROIANO, *Trans. Met. Soc. AIME* **215** (1959) 1048.
12. A. R. TROIANO *Trans. ASM* **52** (1960) 54.
13. A. S. TETELMAN, "Fracture of Solids" (Wiley, New York, 1962) p. 671.
14. J. G. MORTLETT, H. H. JOHNSON and A. R. TROIANO, *J. Iron Steel Inst.* **189** (1959) 37.
15. N. J. PETCH, *Phil. Mag.* **1** (1956) 331.
16. D. P. WILLIAMS and H. G. NELSON, *Met. Trans.* **1** (1970) 63.
17. J. D. FRANDSEN and H. L. MARCUS, *Scripta Met.* **9** (1975) 1089.
18. J. F. LESSAR and W. W. GERBERICH, *Met. Trans.* **7** (1976) 953.
19. T. R. WILSHAW, C. A. RAU and A. S. TETELMAN, *Eng. Fract. Mech.* **1** (1968) 191.
20. J. R. GRIFFITHS and D. R. J. OWEN, *J. Mech. Phys. Solids* **19** (1971) 419.
21. R. O. RITCHIE, J. F. KNOTT and J. R. RICE, *ibid* **21** (1973) 395.
22. W. W. GERBERICH, Y. T. CHEN and C. ST. JOHN, *Met. Trans.* **6** (1975) 1485.
23. J. R. RICE, *Corrosion* **32** (1976) 22.
24. A. H. COTTRELL, "Dislocations and Plastic Flow in Crystals" (Clarendon Press, Oxford, 1953).
25. R. A. ORIANI, "Fundamental Aspects of Stress Corrosion Cracking" (N.A.C.E., Houston, USA, 1969).
26. W. W. GERBERICH and Y. T. CHEN, *Met. Trans.* **6** (1975) 271.
27. R. HILL, "Mathematical Theory of Plasticity" (Clarendon Press, Oxford, 1950).
28. A. J. WANG, *Q. Appl. Mech.* **11** (1954) 427.
29. D. KALDERON, *Proc. Inst. Mech. Eng.* **186** (1972) 341.

30. C. S. KORTOVICH and E. A. STEIGERWALD, *Eng. Fract. Mech.* 4 (1972) 637.
31. C. F. BARTH and E. A. STEIGERWALD, *Met. Trans.* **1** (1970) 3451.
32. C. E. INGLIS, *Trans. Inst. Naval Arch.* **55** (1913) 219.
33. W. K. WILSON, *J. Press. Vess. Technol.* **96** (1974) 293.
34. P. McINTYRE, "Stress Corrosion Cracking and Hydrogen Embrittlement of Iron-Base Alloys", Paper F11, Unieux-Firminy, France (1973).
35. W. G. CLARK, Westinghouse Scientific Paper, No. 73-1E7-MSLRA-P3 (1975).

Received 5 September and accepted 4 October 1978.